International Journal of Pharmaceutics 367 (2009) 140–147

Contents lists available at ScienceDirect

International Journal of Pharmaceutics

journal homepage: www.elsevier.com/locate/ijpharm

Development of novel formulations for Chagas' disease: Optimization of benznidazole chitosan microparticles based on artificial neural networks

Dario Leonardi[a,b], Claudio J. Salomón[a,b], María C. Lamas[a,b,*], Alejandro C. Olivieri[a,c,**]

[a] IQUIR – CONICET, Facultad de Ciencias Bioquímicas y Farmacéuticas, Universidad Nacional de Rosario, Suipacha 531, S2002LRK Rosario, Argentina
[b] Departamento Farmacia, Facultad de Ciencias Bioquímicas y Farmacéuticas, Universidad Nacional de Rosario, Suipacha 531, S2002LRK Rosario, Argentina
[c] Departamento de Química Analítica, Facultad de Ciencias Bioquímicas y Farmacéuticas, Universidad Nacional de Rosario, Suipacha 531, S2002LRK Rosario, Argentina

ARTICLE INFO

Article history:
Received 28 July 2008
Received in revised form
18 September 2008
Accepted 22 September 2008
Available online 30 September 2008

Keywords:
Benznidazole
Chagas' disease
Chitosan
Microparticles
Optimization
Artificial neural networks

ABSTRACT

Benznidazole (BZL) is one of the two therapeutic agents used for the treatment of Chagas' disease. However, the use of BZL in most pharmaceutical preparations and research experiments is still limited due to its low water solubility (0.4 mg/mL). To overcome the dissolution rate-limiting step in oral absorption, chitosan microparticles prepared by the coacervation method were chosen, owing to non-toxicity of the polymer and mild conditions of the method. The influence of process parameters such as encapsulation efficiency, size, yield, and dissolution rate was optimized by using artificial neural networks (ANNs). The optimal conditions were found to be 1.5% (w/v) for the polymer concentration, 6.0% (w/v) for the coacervation agent concentration, 1400.0 rpm for the stirring rate, and 5.0 mL/min for the spraying rate. Confirmation experiments showed good agreement between predicted and experimental values of the optimized properties. These results indicate that ANNs is a valuable tool for the development of optimized BZL chitosan microparticles. To our knowledge it is the first report based on the development of optimized BZL microparticles.

1. Introduction

The group of tropical infectious diseases that are prevalent in the world's least developed nations are known as neglected diseases (Beyrer et al., 2006). Among them, Chagas' disease, caused by the intracellular protozoan parasite *Trypanosoma cruzi*, affects an estimated 20 million people in Latin America, with another 40 million at risk of acquiring the infection (World Health Organization, 2002). It is characterized by an acute phase with detectable parasitemia and acute myocarditis in 8% of cases and a long-lasting chronic phase in which most infected people remain asymptomatic (Cuellar et al., 2003; Bustamante et al., 2007). Chagas' disease is also an emerging opportunistic infection among immunocompetent patients (Cordova et al., 1992). In addition, it was reported recently a dissemination of this parasitic disease through contaminated blood transfusions in North America, and Europe (Leiby et al., 2002). Although many efforts have been carried out in order to develop new strategies to reduce or minimize the morbidity and mortality associated with Chagas' disease, to date a novel and successful chemotherapy for the treatment is lacking.

BZL liposomal formulations prepared by mixing a solution of lipids in chloroform–methanol and BZL dissolved in dimethylsulfoxide or in a mixture of chloroform, methanol and water were described (Morilla et al., 2002). Despite the frequent use of these solvents for liposomal formulations, there is some concern especially in the case of chloroform, a carcinogenic agent (Ran and Yalkowsky, 2003). Later, it was found that, BZL delivery was not greatly increased after incorporation in these liposomes (Morilla et al., 2004).

Recently, our group developed oral and parenteral formulations of BZL, using non-toxic co-solvents systems. It was revealed that these PEG 400-based systems were able to increase the BZL solubility up to 10 mg/mL and exhibited an excellent trypanocide activity (Lamas et al., 2006). To the best of our knowledge, no additional BZL formulations have been developed. Thus, an urgent need exists for the design and development of safe and effective delivery systems for BZL, aimed at reducing the administered dose to improve the absorption (Mizoe et al., 2007).

Preparation and optimization of chitosan (CH) microparticulate systems prepared by coacervation method was analyzed employing

* Corresponding author at: Departamento Farmacia, Facultad de Ciencias Bioquímicas y Farmacéuticas, Universidad Nacional de Rosario, Suipacha 531, S2002LRK Rosario, Argentina. Tel.: +54 341 4804592; fax: +54 341 4375315.
** Corresponding author at: IQUIR – CONICET, Facultad de Ciencias Bioquímicas y Farmacéuticas, Universidad Nacional de Rosario, Suipacha 531, S2002LRK Rosario, Argentina. Tel.: +54 341 4804592; fax: +54 341 4375315.
E-mail addresses: mlamas@fbioyf.unr.edu.ar (M.C. Lamas), aolivier@fbioyf.unr.edu.ar (A.C. Olivieri).

0378-5173/$ – see front matter © 2008 Elsevier B.V. All rights reserved.
doi:10.1016/j.ijpharm.2008.09.036

Table 1
Plackett–Burman design build for factor selection.

Experiments	Factors[a]				Responses[b]				
	PC (%, w/v)	NaOH (%, w/v)	SR (rpm)	SPR (mL/min)	S (μm)	M	Y (%)	EE (%)	D_r (Q_{30}) (%)
1	0.30	3.00	1000.00	15.00	200	1	80	63.12	82.14
2	0.30	5.00	1000.00	5.00	10	1	78	68.23	98.71
3	3.00	5.00	1000.00	15.00	400	1	75	66.39	75.87
4	0.30	5.00	200.00	15.00	300	1	78	63.24	79.15
5	3.00	3.00	1000.00	5.00	30	1	31	67.31	97.33
6	3.00	5.00	200.00	5.00	250	1	66	69.91	80.61
7	0.30	3.00	200.00	5.00	90	1	54	70.15	87.59
8	1.65	4.00	600.00	10.00	200	1	61	61.16	83.27
9	1.65	4.00	600.00	10.00	180	1	63	63.39	85.11
10	3.00	3.00	200.00	15.00	500	1	28	59.91	73.77

[a] PC: polymer concentration, SR: stirring rate, NaOH: coacervation agent solution concentration, SPR: spraying rate.
[b] S: mean size, EE: encapsulation efficiency, D_r (Q_{30}): dissolution rate, Y: yield, M: morphology.

artificial neural network (ANN) (Ya-I et al., 2007). The influence of several factors in the microparticle formulation was evaluated, in order to distinguish those which have a significant effect on four responses: yield, dissolution rate, encapsulation efficiency, and size of the microparticles.

The aim of this work was to study the potential of BZL microparticules for the development of fast-release systems. The absorption of most orally administered drugs in the gastro-intestinal tract can be related to their solubility. This parameter can be modifying by microencapsulation process with biocompatible polymers such as CH (Daniel-Mwanbete et al, 2004).

The dissolution profile of BZL from CH microparticules was compared with the pure drug. The morphology of the polymeric systems was studied using scanning electron microscopy (SEM). Furthermore, and X-ray powder diffraction were used to investigate possible interactions between the components. Several formulations have been performed to confirm the optimization values. Experiments showed good agreement between predicted and experimental values of the optimized properties of the microparticles.

2. Materials and methods

2.1. Materials

BZL was a gift from Roche Laboratory (Roche, Brazil) and CH was supplied by Aldrich Chemical Co. (Milwaukee, WI, USA). All other chemicals were of analytical grade.

2.2. Methods

2.2.1. Preparation of BZL–CH microparticles

Microparticles were prepared by the coacervation method (ionic gelation), performed according to the following procedure: BZL (100 mg) was dissolved at room temperature in acetic acid (25 mL) and water (25 mL). A given amount of CH (0.3–3.0%, w/v) was dispersed in the acidic solution. The resulting suspension was stirred to allow the complete CH dissolution in the acidic medium.

The drug–polymer solution was sprayed at several velocities (5–15 mL/min) over NaOH solutions (3.00–5.00%, w/v). All experiments were done at 25 °C, fixing a stirring time (2 h) required to complete the coacervation. The stirring rate was kept stable during this procedure. Samples were washed and centrifuged twice, and finally collected in a drying chamber at 40 °C. Conditions of preparation procedure are detailed in Table 1.

2.2.2. Yield determination

The yield was calculated as the ratio between the experimental weight of the product and the sum of the weights of all components

$$\text{yield}\,(\%) = 100\left[\frac{W_{\text{product}}}{W_{\text{BZL}} + W_{\text{CH}} + W_{\text{NaOH}}}\right] \quad (1)$$

where W_{product} is the weight of the obtained microparticles and W_{BZL}, W_{CH}, and W_{NaOH} are the weights of BZL, CH, and Na(OH) respectively.

2.2.3. Determination of BZL content in microparticles

The encapsulation efficiency (EE) has been determined by the following procedure.

Microparticles were dissolved in 0.1N HCl for 24 h, and the amount of loaded drug was analyzed by spectrophotometric measurements at 322 nm using a LKB-Pharmacia UV spectrophotometer, according to

$$\text{encapsulation efficiency}\,(\%) = 100\left(\frac{W_{\text{BZL}}}{W_{\text{t}}}\right) \quad (2)$$

where W_{BZL} is the actual BZL content and W_{t} is theoretical BZL content in the microparticles.

2.2.4. Morphological analysis and size determination

The morphological analysis and mean diameters of the microparticles were determined using scanning electron microscopy (SEM) (Leitz SEM AMR 1600T). Samples were previously sputter-coated with a gold layer in order to make them conductive.

2.2.5. Dissolution studies

All of the BZL–CH microparticles were subjected to dissolution assays in an USP Standard Dissolution Apparatus (Hanson Research SR8 Plus, Chatsworth, CA, USA), equipped with a rotational paddle (50 rpm). The dissolution medium (900 mL of 0.1N HCl) was maintained at 37 °C. A dispersion powder of microparticles containing BZL was introduced into the flasks, and the time counter was set to zero. At different time intervals, samples of 5 mL were taken through a filter, and the amount of BZL released was determined. It was found that CH did not interfere with the assay at the working wavelength.

2.2.6. Software

Design Expert version 7.0.3 (Stat-Ease Inc., Minneapolis, MN, USA) was used for performing the experimental design, polynomial fitting and ANOVA results. ANN training was done using the MATLAB 7.0 Neural Network Toolbox (The Mathworks, Natick, MA,

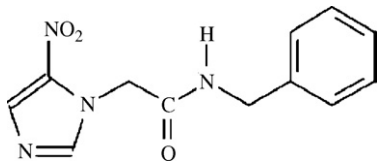

Fig. 1. Chemical structure of BZL.

Table 2
Values of p obtained for the different factors on the five responses.

	S	M	EE	D_r (Q_{30})	Y
Model	0.0062	0.0000	0.1344	0.0031	0.0246
PC	0.0147		0.8625	0.0147	0.0128
SR	0.0239		0.7944	0.0036	0.0662
SPR	0.0019		0.0255	0.0009	0.0898
NaOH	0.3772		0.3323	0.1980	0.0097

USA, 2007) while desirability calculations were performed with in-house MATLAB 7.0 routines.

3. Results and discussion

3.1. Screening phase

A satisfactory microparticle formulation depends on many factors, and therefore an expanded Plackett–Burman design was built for estimating the main factors affecting its properties (Talpur et al., 2008). The analyzed factors were: CH concentration, NaOH concentration, stirring rate and spraying rate. Each of these factors was evaluated at three levels (a triplicate central point was added to the Plackett–Burman design in order to provide higher information content for the analysis, see Table 1). The factor ranges were selected based on prior knowledge about the system under study. The evaluation consisted in analyzing the responses in all the conditions quoted in Table 1. It should be noticed that an excess of NaOH is necessary to secure the microparticles formation; therefore the NaOH concentration was higher than the CH concentration in all the experiments.

The five analyzed responses were: yield, morphology, size, encapsulation efficiency and micropaticle dissolution rate (based on the Q_{30} value, which is defined as the drug concentration dissolved after 30 min). Morphology is a categorical response, and hence values of 1 or 0 were assigned to analyze this response: a value of 1 indicates the tendency to form microspheres, while a value of 0 implies a tendency to form microparticles having different non-spherical forms (Fig. 1).

An ANOVA test was applied to the experimental data corresponding to the design of Table 1, using the effect of the dummy variables to obtain an estimate of standard errors in the coefficients. As a conclusion of this analysis , all factors were significant (values of $p < 0.05$ as quoted in boldface in Table 2). The results also revealed no significant relationship between the studied factors and the response M: in all cases studied the morphology corresponded to quasi-spherical particles. Half-normal probability plots for the analyzed responses were built (results obtained for dissolution rate (D_r), size (S), and yield (Y) are shown in Fig. 2). These results allowed to reach an analogous conclusion regarding the values collected in Table 2.

3.2. Response surface design

It has been established that the studied factors had a significant influence on three of the analyzed responses. Then, a systematic optimization procedure was carried out using response surface methods (RSM), in order to estimate the values of the most important factors leading to the best compromise between maximum dissolution rate, yield and encapsulation efficiency on one hand, and minimum size on the other (Almeida Becerra et al., 2008). A central composite design was employed for applying the RSM, consisting in 27 experiments ($4^2 = 16$ two-level four-factor points, $4 \times 2 = 8$ axial points and a triplicate central point), which were combinations of the factors in the following ranges: 0.3–4.35% (w/v) polymer concentration; 2–5% (w/v) Na(OH) solution concentration; 200–1400 rpm stirring rate and 5–15 mL/min spraying rate (Table 3).

However, unsatisfactory fit was achieved using this RSM chemometric tool (Table 4). The only model which showed a non-significant lack of fit was the one concerning the encapsulation efficiency; in the remaining cases the residual errors significantly exceeded the pure error, and therefore the models showed significant lack of fit. Under these circumstances, it is advisable to seek for additional mathematical models which may be more appropriate.

Based on these results, the optimization cannot be accomplished by means of quadratic or cubic polynomials, because of the poor reliability of the fitted models. An attractive alternative is the use of artificial neural networks, a methodology which was recently

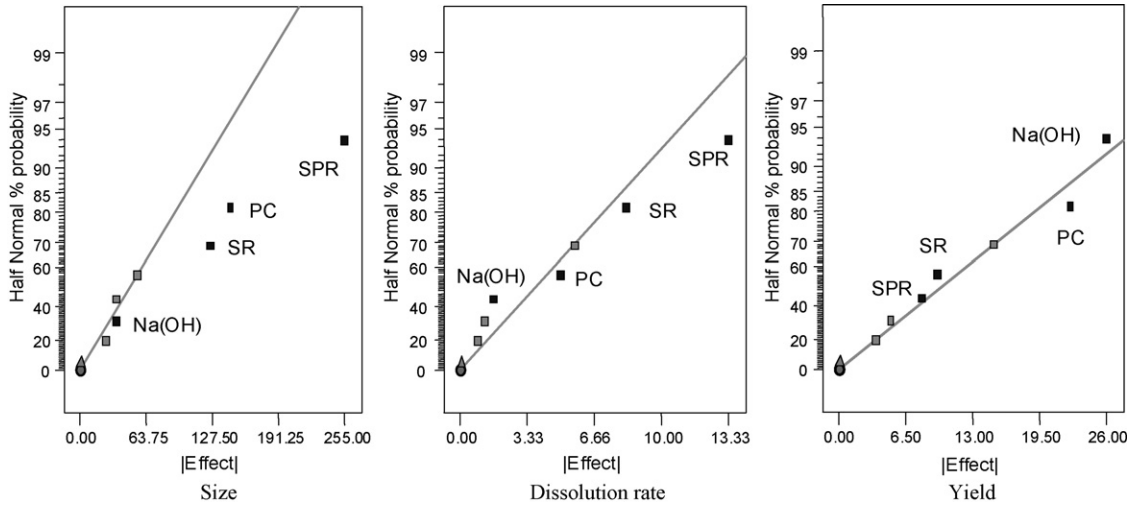

Fig. 2. Half-normal probability plots for the responses S, D_r, and Y as indicated.

Table 3
Central composite design used for the optimization of the responses.

Std	Run	Polymer concentration (%, w/v)	Na(OH) solution concentration (%, w/v)	Stirring rate (rpm)	Spraying rate (mL/min)	Size (μm)	Yield (%)	Encapsulation efficiency (%)	Dissolution rate (%)
19	1	1.65	2.00	600.00	10.00	30	58	61	97
1	2	0.30	3.00	200.00	5.00	80	65	70	88
2	3	3.00	3.00	200.00	5.00	140	35	55	79
7	4	0.30	5.00	1000.00	5.00	15	80	70	99
5	5	0.30	3.00	1000.00	5.00	30	77	68	95
6	6	3.00	3.00	1000.00	5.00	40	35	52	96
11	7	0.30	5.00	200.00	15.00	280	76	64	82
10	8	3.00	3.00	200.00	15.00	520	30	50	75
16	9	3.00	5.00	1000.00	15.00	410	73	65	77
8	10	3.00	5.00	1000.00	5.00	70	71	78	89
18	11	4.35	4.00	600.00	10.00	610	24	41	67
9	12	0.30	3.00	200.00	15.00	400	64	57	73
22	13	1.65	4.00	1400.00	10.00	80	62	40	87
27	14	1.65	4.00	600.00	10.00	180	60	62	85
26	15	1.65	4.00	600.00	10.00	200	65	60	81
15	16	0.30	5.00	1000.00	15.00	70	80	61	90
14	17	3.00	3.00	1000.00	15.00	100	42	30	86
12	18	3.00	5.00	200.00	15.00	180	75	56	80
17	19	1.05	4.00	600.00	10.00	120	80	63	82
13	20	0.30	3.00	1000.00	15.00	220	78	62	80
21	21	1.65	4.00	200.00	10.00	120	65	49	80
24	22	1.65	4.00	600.00	20.00	500	73	40	71
23	23	1.65	4.00	600.00	10.00	180	63	67	85
25	24	1.65	4.00	600.00	10.00	200	60	60	83
3	25	0.30	5.00	200.00	5.00	400	61	66	70
20	26	1.65	6.00	600.00	10.00	120	63	62	80
4	27	3.00	5.00	200.00	5.00	270	64	67	78

employed for the modeling of properties in multiresponse optimization cases (Chegini et al., 2008).

3.2.1. Artificial neural networks

Artificial neural networks are mathematical models having the ability to learn the correlation between experimental data (input) and response (output) values by means of an iterative mechanism of test and error (Zupan and Gasteiger, 1999). Neural networks are composed of basic units called neurons or nodes distributed in different layers. In this work, a neural network involving three layers was employed: input, hidden and output layer (Fig. 3). The output layer was designed with four neurons, corresponding to the size, encapsulation efficiency, yield and dissolution rates. The inputs were the polymer concentration, the NaOH concentration, the stirring rate and the spraying rate. A multiresponse optimization was then applied to obtain minimum size, and maximum yield, encapsulation efficiency and dissolution rate.

As in the nervous system, each artificial neuron receives the output from the previous neurons, and each connection between neurons carries an assigned weight. For the network training, the experimental data (X) were entered into the input layer, and propagated through the network. Each neuron of the hidden layer

Table 4
Analysis of variance (ANOVA).

Source	Sum of squares	DF	Mean square	*F* value	Prob > *F*
Size					
Residual	392,550	22	17843		
Lack of fit	392,150	19	20639	154.8	0.0007 significant
Pure error	400	3	133		
Total correlation	709,516	26			
Yield					
Residual	1,080	16	67		
Lack of fit	1,062	13	81	13.6	0.027 significant
Pure error	18	3	6		
Total correlation	6,528	26			
Encapsulation efficiency					
Residual	1,553	22	70		
Lack of fit	1,520	19	80	7.3	0.063 not significant
Pure error	32	3	11		
Total correlation	3,110	26			
Dissolution rate					
Residual	834	22	38		
Lack of fit	823	19	43	11.8	0.032 significant
Pure error	11	3	3.7		
Total correlation	1,758	26			

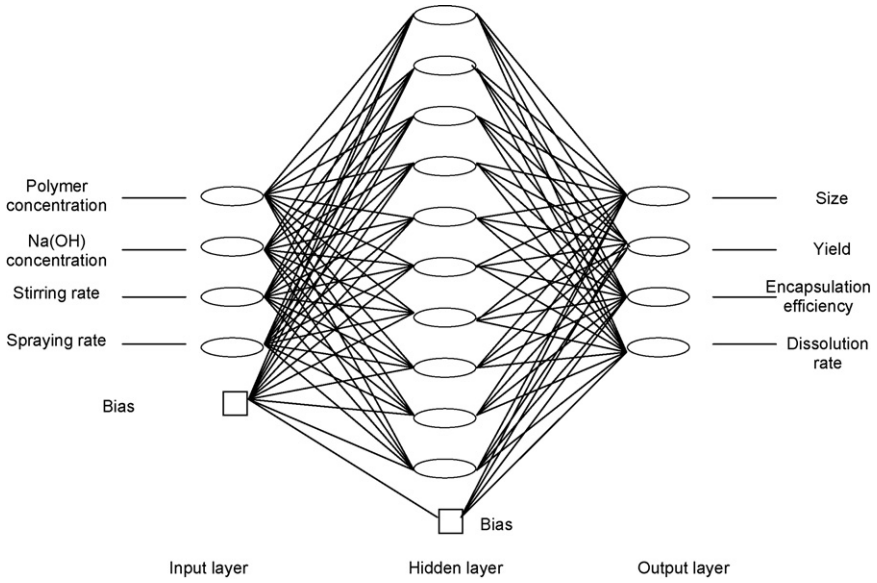

Fig. 3. Neural networks involving three layers: input, hidden and output layer.

received and added the outputs from all of the neurons in the input layer. After that, the resulting summation was analyzed through a transfer function, the output for the *j*th neuron in the hidden layer (y_j) equals to

$$y_j = \frac{1}{1 + e^{net_j}} \tag{3}$$

where net_j is the net input to the *j*th neuron in the hidden layer, which is given by the expression

$$net_j = \sum_{i=1}^{n} w_{ji} x_i \tag{4}$$

where *n* is the number of neurons in the input layer, w_{jt} is the connection weight from the *i*th neuron in the input layer to the *j*th neuron in the hidden layer and x_i is the input to the *i*th neuron in the input layer.

For both the input and hidden layers, two bias neurons were used; these neurons are connected to all the neurons in the next layer, but none in the previous layer and they always emit 1. Thus, the weights connected to the bias neuron are added directly to the combined sum of the remaining weights. During the network training, a back-propagation learning algorithm was used to compute the weights. The error between the output vector of the network (out_{calc}) and the experimental vector ($out_{\exp}$) was calculated, and then all weights were corrected throughout the entire network from the last layer to the first one. After weight correction, the procedure was repeated until an acceptable error was reached. The error was calculated as the root mean square error of training (*RMSET*), according to

$$RMSET = \frac{\sqrt{\sum (out_{calc} - out_{\exp})^2}}{I} \tag{5}$$

where *I* is the total number of responses.

3.2.2. Bayesian regularization

The overtraining problem is quite common in the field of ANN, and is related to the number of network training cycles: after a certain number of cycles, the network may model not only the useful signal, but also the background noise (Sjöberg, 1995). This problem has been previously discussed in several works, and various proposals exist in order to solve it, employing different techniques such as Bayesian regularization, early stopping, optimal brain damage, and optimal brain surgeon (Pedersen and Hansen, 1994; Sjöberg and Ljung, 1992; Le Cun et al., 1990; Hassibi and Stork, 1993).

In this work, we have selected Bayesian regularization to avoid the overtraining problem, because this technique allows one to train the network model using the entire training set of objects. This is useful in view of the fact that the training set has a specific statistical design, hence it is not advisable to remove samples to be used as an independent monitoring set, as is regularly done in early stopping. Regularization aims at minimizing a combination of the square error and the sum of network weights

$$MSE_{\text{reg}} = \gamma\, MSE + (1 - \gamma) MSW \tag{6}$$

where MSE_{reg} is the regularized mean square error, *MSE* is the square of the *RMSET* value commented above, *MSW* is the mean sum of squares of all network weights, and γ is the so-called regularization parameter. In Bayesian regularization, the weights and biases of the network are assumed to be random variables with specified distributions, while the regularization parameter is related to the variance associated with these distributions (Pedersen and Hansen, 1994). Using MSE_{reg} as performance function causes the network to have smaller weights and biases, and these forces the model response to be smoother and less likely to overfit.

The present network was trained for the studied properties using the experimental design of Table 3 as input signals, and the values of size, encapsulation efficiency, yield and dissolution rate as output values. The number of neurons in the hidden layer was selected based on the results obtained on *RMSET* values and the number of effective parameters of the net (Pedersen and Hansen, 1994).

Table 5 showed that these two latter parameters tend to stabilize beyond 10 hidden neurons, and therefore this latter number was subsequently employed. Training a Bayesian regularization network with this architecture (i.e., 4 input, 10 hidden and 4 output neurons) leads to an overall *RMSET* value of 0.25 units (after scaling all input and output variables to be in the range from −1 to 1). The individual *RMSET* values for each of the four analyzed responses were all satisfactory: 0.16, 0.32, 0.26 and 0.26 for size, encapsula-

Table 5
RMSET and number of parameters when training several ANNs with different numbers of hidden neurons.

Neurons in the hidden layer	*RMSET*[a]	Effective parameters	Total parameters
2	1.6	18	22
4	1.1	35	40
6	0.8	45	58
8	0.4	64	76
10	0.25	76	94
12	0.25	80	112
14	0.25	82	130

[a] The *RMSET* values given in this table refer to the overall *RMSET* for all four responses, after scaling all variables in the range from −1 to 1.

tion efficiency, yield and dissolution rate respectively. These results were attained after 220 training cycles.

3.2.3. Multiple response optimization

When a simple response is being analyzed, the model analysis indicates areas in the design region where the system is likely to give desirable results. However, when several responses are needed to be simultaneously optimized, the desirability function can be employed, which is a function of more than one response (Espinoza-Escalante et al., 2007; Vera Candioti et al., 2006).

The desirability function intends to include the priorities and desires of the researcher when building the optimization procedure. The procedure involves creating a function for each individual response (d_i) and finally obtaining a global function D that should be maximized, choosing the best conditions of the designed vari-

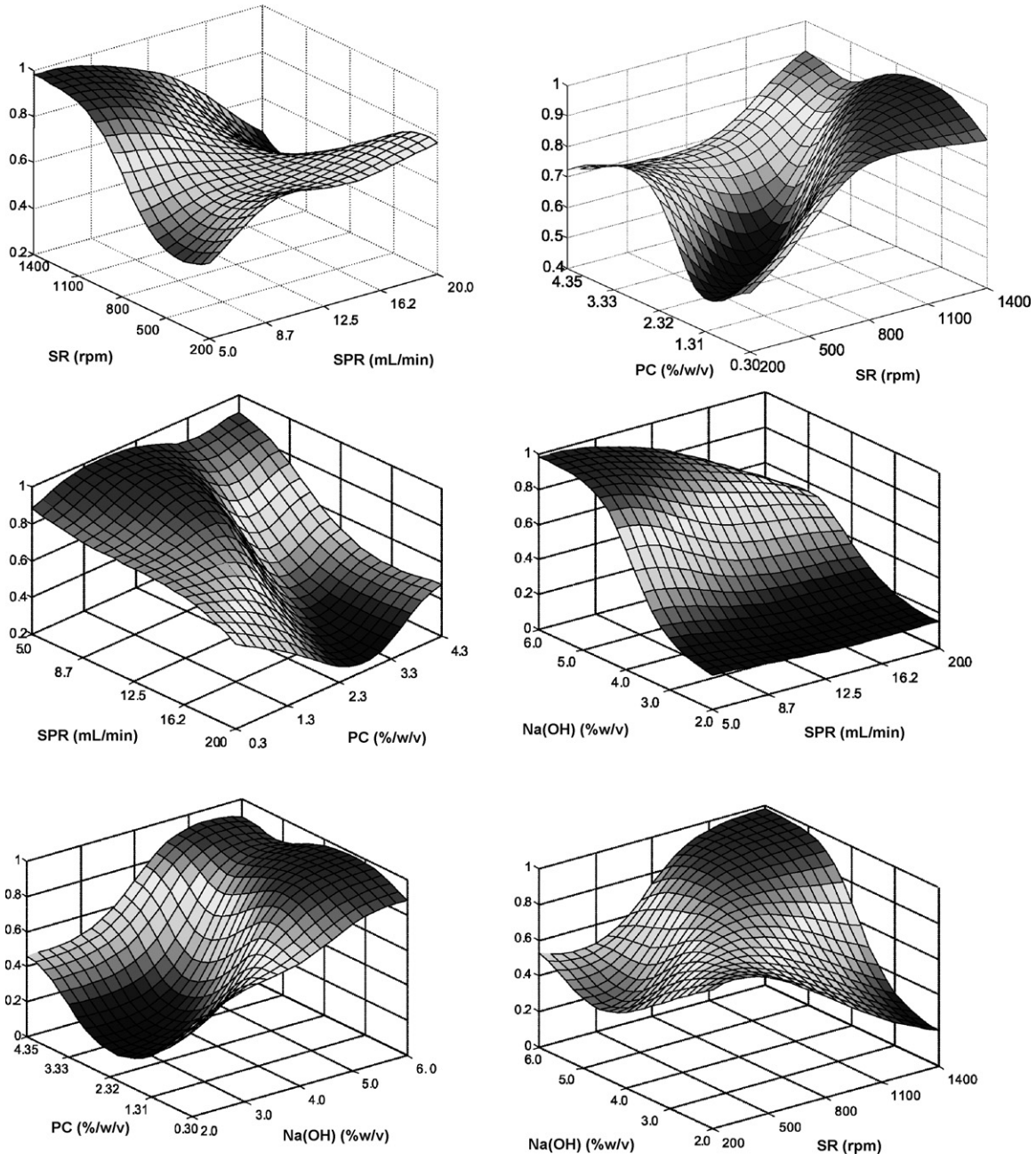

Fig. 4. Response surface plots of pairs of factors (PC/SR; SPR/PC; Na(OH) w/v/SPR; PC/Na(OH) w/v; Na(OH) w/v/SR) with the remaining ones at their optimum values.

Table 6
Comparison between expected and experimental values obtained with optimized conditions.

Response	Predicted value	Experimental value
Size	17.0	8.5
Encapsulation efficiency	78.8	79.1
Yield	76.8	78.0
Dissolution rate (Q_{30})	98.6	98.5

ables. The function D ranges from 0 (value totally undesirable) to 1 (all responses are in a desirable range simultaneously) and is defined by Eq. (7), where $d_1, d_2, \ldots, d_N$ corresponds to the individual desirability function for each response being optimized

$$D = \left[\prod_{n=1}^{N} (d_n)^{w_n}\right]^{1/\sum_{n=1}^{N} w_n} \quad (7)$$

where w_n is a weight which controls the relative importance of each of the analyzed factors. In the present work, all weights were set to unity, and hence a simplified version of Eq. (7) was employed

$$D = \left[\prod_{n=1}^{N} d_n\right]^{1/N} \quad (8)$$

Four responses, as suggested by the analysis of the effect discussed above, were simultaneously optimized: minimum size and maximum dissolution rate, encapsulation efficiency and yield are desirable. After the optimization procedure was carried out, and adequate models were found for each of these responses, a response surface for the each desirability function was built as a function of the influencing responses S, EE, Y and D_r. Fig. 4 shows the surface of D as a function of selected pairs of factors. The optimum D value was found to be 0.98, corresponding to the following values of the influencing factors: polymer concentration, 1.5% (w/v), NaOH concentration, 6.0% (w/v), stirring rate, 1400.0 rpm and spraying rate, 5.0 mL/min. The obtained value of D, ca. 98% of the best possible value for this parameter, represents an excellent compromise among the analyzed responses.

4. Experimental verification

The optimal conditions for the preparation of microparticles were verified by an additional independent experiment. The optimal combination assayed, as given by the ANN study discussed in the previous section, provided experimental results which were in agreement with the ANN-predicted optimum values, with differences which were on the order of the analytical measurement error (Table 5). These interesting findings provided a strong confidence in that the applied optimization procedure was leading to reliable values of the factors influencing the presently studied formulation. They also confirmed the already known ability of artificial neural networks as universal approximators to multivariate non-linear functions. These chemometric tools were highly valuable when traditional response surface analyzed based on polynomial regression fail to adequately model the factor–response relationship under investigation (Table 6).

Some of the optimum factor values could be explained by considering the physicochemical parameters of the ionic gelation procedure (coacervation method). For example, the concentration of CH (PC) had a significant effect on the EE. This was ascribed to the fact that low concentrations of PC may lead to insufficient ionic interaction to produce monolithic microparticles, and large pores sizes permitted the drug to diffuse out during the manufacturing process. Higher concentrations of CH provided increasing ionic interactions and thus an increased degree of entrapment. The drug/polymer mass ratio of the BZL-microparticles could dramatically affect the drug release rate (Q_{30}). In this particular case the Q_{30} values are 48.51% of drug release from pure drug and 98% of drug release from the microparticles.

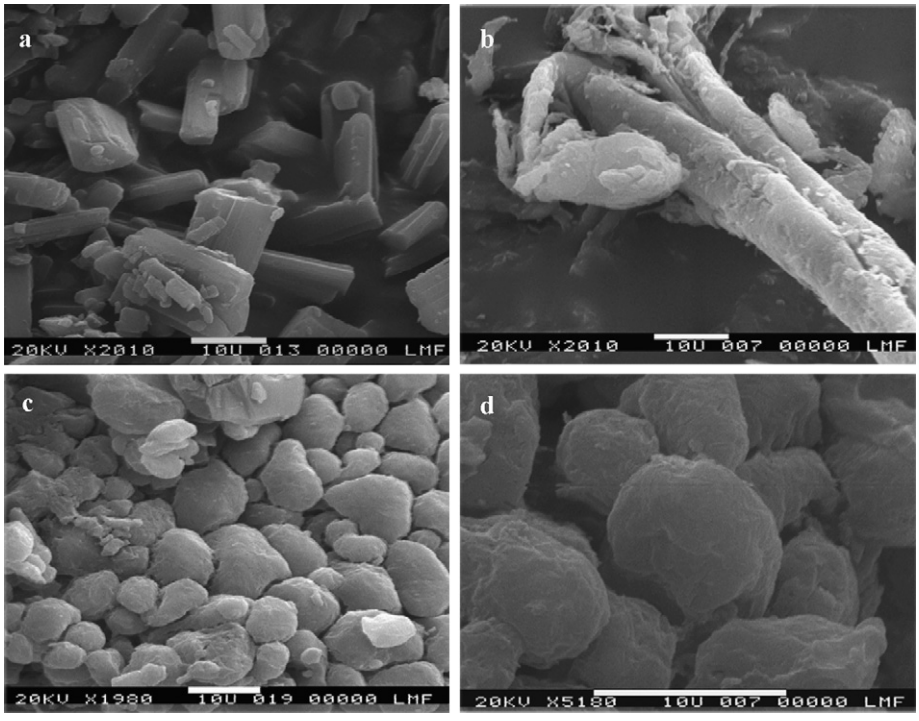

Fig. 5. Photographs (scanning electron microscopy) (SEM): (a) drug, (b) polymer, and (c and d) microparticles obtained at two magnifications, as indicated.

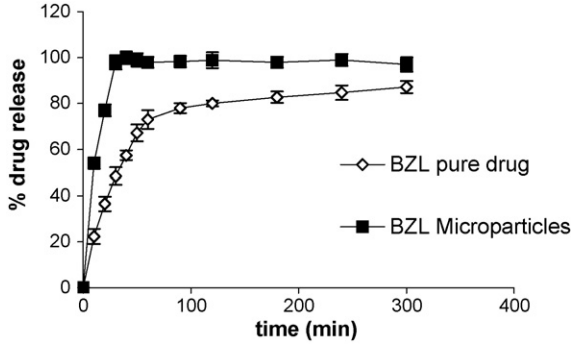

Fig. 6. Dissolution profiles of pure BZL and microparticles in the optimal conditions.

Moreover, the NaOH concentration also affected the effectiveness of the coacervation procedure, increasing the ionic interaction and modifying the pH values. High SR and SPR allowed obtaining particles with minimum sizes, without the formation of beads.

The morphologic study of polymer, isolated drug, and obtained microparticles was shown in Fig. 5 by resorting to SEM analysis. Typical micrographs for BZL–CH microparticles were presented at two different magnifications. As could be appreciated, the polymer was formed by blocks of different forms and sizes. On the other hand, the microparticles obtained in the optimal conditions had spherical shapes and a relatively uniform size, both properties which are highly desirable for the present formulation.

The dissolution profile for a formulation obtained in the selected conditions was contrasted against isolated BZL without any treatment (Fig. 6). As could be seen, the microparticle formulation showed an enhanced dissolution rate for BZL in comparison with the drug alone, confirming that the formation of microparticles conferred improved dissolution properties to the drug.

5. Conclusions

This work has demonstrated that the properties of BZL–CH microparticles could be greatly improved by rationally analyzing the influence of different parameters in the formulation. The analysis was composed of the following four phases: (1) screening the influential factors with a Plackett–Burman design, (2) modeling the responses using artificial neural networks, (3) finding the optimal conditions through desirability considerations, and (4) verifying the optimal formulation. This methodology has been proved to be very efficient in decreasing the particle size and increasing the encapsulation efficiency, yield and dissolution rate of BZL. The optimal combination of the microencapsulating materials was found to be 1.5% (w/v) polymer concentration, 6.0% (w/v) NaOH solution concentration, 1400 rpm stirring rate and 5 mL/min spraying rate.

Acknowledgments

D.L. is gratefull to CONICET for a Post-Doctoral Fellowship. University of Rosario, CONICET (Consejo Nacional de Investigaciones Científicas y Técnicas, Project Nos. PIP 5303 and 5744), Bunge & Born Foundation (Argentina) and ANPCyT (Agencia Nacional de Promoción Científica y Tecnológica, Project No. PICT 25825) are gratefully acknowledged for financial support.

References

Almeida becerra, M., Erthal Santelli, R., Padua Oliveira, E., Silveira Villar, L., Escaleira, L.A., 2008. Response surface methodology (RSM) as a tool for optimization in analytical chemistry. Talanta 76, 965–977.
Beyrer, C., Villar, J.C., Suwanvanichkij, V., Singh, S., Baral, S., Mills, E.J., 2006. Neglected diseases, civil conflicts, and the right to health. Lancet 370, 619–627.
Bustamante, J.M., Lo Presti, M.S., Rivarola, H.W., Fernández, A.R., Enders, J.E., Fretes, R.E., Paglini-Oliva, P., 2007. Treatment with benznidazole or thioridazine in the chronic phase of experimental Chagas' disease improves cardiopathy. Int. J. Antimicrob. Agents 29, 733–737.
Chegini, G.R., Khazaei, J., Ghobadian, B., Goudarzi, A.M., 2008. Prediction of process and product parameters in an orange juice spray dryer using artificial neural networks. J. Food Eng. 84, 534–543.
Cordova, E., Boschi, A., Ambrosioni, J., Cudos, C., Corti, M., 1992-2007. Reactivation of Chagas' disease with central nervous system involvement in HIV-infected patients in Argentina. Int. J. Infect. Diseases 12, 587–592.
Cuellar, M., Salas, C., Cortes, M., Morello, A., Maya, J., Preite, M., 2003. Synthesis and in vitro trypanocide activity of several polycyclic drimanequinone derivatives. Bioorg. Med. Chem. 11, 2489–2497.
Daniel-Mwanbete, K., Torrado, S., Cuesta-Bandera, C., Ponce-Gordo, F., Torrado, J., 2004. The effect of solubilization on the oral bioavailability of three benzimidazole carbamate drugs. Int. J. of Pharm. 272, 29–36.
Espinoza-Escalante, F.M., Pelayo-Ortiz, C., Gutierrez-Pulido, H., Gonzalez-A Ivarez, V., Alcaraz-Gonzalez, V., Bories, A., 2007. Multiple response optimization analysis for pretreatments of Tequila's stillages for VFAs and hydrogen production. Bioresource Technol. 99, 5822–5829.
Hassibi, B., Stork, D.G., 1993. Second order derivatives for network pruning: optimal brain surgeon. In: Proceedings of the NIPS 5,164, San Mateo, California, pp. 164–172.
Lamas, M.C., Villaggi, L., Nocito, I., Bassani, G., Leonardi, D., Pascutti, F., Serra, E., Salomón, C., 2006. Development of parenteral formulations and evaluation of the biological activity of the trypanocide drug benznidazole. Int. J. Pharm. 307, 239–243.
Le Cun, Y., Denker, J.S., Solla, S.A., 1990. In: Touretzsky, D. (Ed.), Optimal Brain Damage, Advances in Neural Information Processing Systems. Morgan Kaufmann, Denver, pp. 598–605.
Leiby, D.A., Herron Jr., R.M., Read, E.J., Lenes, B.A., Stumpf, R.J., 2002. *Trypanosoma cruzi* in Los Angeles and Miami blood donors: impact of evolving donor demographics on seroprevalence and implications for transfusion transmission. Transfusion 42, 549–555.
Mizoe, T., Beppu, S., Ozeki, T., Okada, H., 2007. One step preparation of drug-containing microparticles to enhance the dissolution and absorption of poorly water-soluble drugs using a 4 fluid nozzle spray drier. J. Control. Release 120, 205–210.
Morilla, M.J., Benavidez, P., Lopez, M.O., Bakas, L., Romero, E.L., 2002. Development and in vitro characterization of a benznidazole liposomal formulation. Int. J. Pharm. 249, 89–99.
Morilla, M.J., Montanari, J.A., Prieto, M.J., Lopez, M.O., Petray, P.B., Romero, E.L., 2004. Intravenous liposomal benznidazole as trypanocidal agent: increasing drug delivery to liver is not enough. Int. J. Pharm. 278, 311–318.
Pedersen, M.W., Hansen, L.K., 1994. Recurrent networks: second order properties and pruning. Proc. Neural Inform. Process. Syst. 7, 673–680.
Ran, Y., Yalkowsky, S.H., 2003. Halothane, a novel solvent for the preparation of liposomes containing 2-4-amino-3-methylphenyl benzothiazole (AMPB), an anticancer drug: a technical note. AAPS Pharm. Sci. Technol. 4, 1–5.
Sjöberg, J., 1995. Non-linear system identification with neural networks, Ph.D. Thesis. Dept. of Electrical Engineering, Linköping University, Sweden.
Sjöberg, J., Ljung, L., 1992. Overtraining, regularization and searching for minimum in neural networks. In: Preprint IFAC Symposium on Adaptive Systems in Control and Signal Processing, Grenoble, France, pp. 669–674.
Talpur, F.N., Bhanger, M.I., Rahman, A.U., Zuhra Memon, G., 2008. Application of factorial design in optimization of anion exchange resin based methylation of vegetable oil and fats. Innovative Food Sci. Emerging Technol. 9, 608–613.
Vera Candioti, L., Robles, J.C., Mantovani, V.E., Goicoechea, H.C., 2006. Multiple response optimization applied to the development of a capillary electrophoretic method for pharmaceutical analysis. Talanta 69, 140–147.
World Health Organization, 2002. Control of Chagas' disease. Tech. Rep. Ser. 905, 1–109.
Ya-I, H., Yu-Hsiu, C., Chien-Chih, Y., Tong-Rong, T., Thau-Ming, C., 2007. Microencapsulation of extract containing shikonin using gelatin–acacia coacervation method: a formaldehyde-free approach. Colloids Surf. B: Biointerf. 58, 290–297.
Zupan, J., Gasteiger, J., 1999. Neural Networks in Chemistry and Drug Design, 2nd edition. Wiley VCH, Weinheim.